Cement and Concrete Research 38 (2008) 1119–1125

Contents lists available at ScienceDirect

Cement and Concrete Research

journal homepage: http://ees.elsevier.com/CEMCON/default.asp

The influence of mineralogical, chemical and physical properties on grindability of commercial clinkers with high MgO level

Vládia Cristina G. de Souza [a,*], Jair Carlos Koppe [a], João F.C.L. Costa [a], André Luís Marin Vargas [b], Eduardo Blando [b], Roberto Hübler [b]

[a] Department of Mining Engineering, Universidade Federal do Rio Grande do Sul, DEMIN/UFGS, Av. bento Gonçalves, 9500, Prédio 75, Setor 4, CEP 91509-900, Porto Alegre, Brazil
[b] GEPSI, faculdade de física da Pontifícia, Instituto de física da PUCRS, Universidade Católica do Rio Grande do Sul, Av. Ipiranga 6681, P.O., CEP 90619-900, Porto Alegre, Brazil

ARTICLE INFO

Article history:
Received 8 June 2006
Accepted 27 February 2008

Keywords:
Clinker
Comminution
Nanohardness
Trace metals

ABSTRACT

This research investigates various methods able to identify possible mineralogical, physical and chemical influences on the grindability of commercial clinkers with high MgO level. The aim of the study is to evaluate the hardness and elastic modulus of the clinker mineral phases and their fracture strength during the comminution processes, comparing samples from clinkers with low MgO level (0.5%) and clinkers with elevated MgO levels (>5.0%). The study of the influence of mineralogical, chemical and physical properties was carried out using several analytical techniques, such as: optical microscopy, X-ray diffraction with Rietveld refinement (XRD) and X-ray fluorescence (XRF). These techniques were useful in qualifying the different clinker samples. The drop weight test (DWT) and the Bond ball mill grindability test were performed to characterize the mechanical properties of clinkers. Nanoindentation tests were also carried out. Results from the Bond ball mill grindability test were found to be related to the hardness of the mineral phase and to mineralogical characteristics, such as type and amount of inclusions in silicates, belite and alite crystals shape, or microcracked alites. In contrast, the results obtained by the DWT were associated to the macro characteristics of clinkers, such as porosity, as well as to the hardness and mineralogical characteristics of belite crystals in clusters. Hardness instrumented tests helped to determine the Vickers hardness and elastic modulus from the mineral phases in commercial clinkers and produced different values for the pure phases compared to previous publications.

1. Introduction

The knowledge of the mechanical properties of clinker minerals directly assists in controlling and optimizing the manufacturing processes and grinding of clinkers, as well as the quality control of the concrete and cements produced as a result. Previous studies in modeling and simulation of concrete and cement microstructures have demonstrated what can be achieved in the field of quality control, via the use of typical applications [1]. Clinker breakage strength, its hardness and elastic modulus provide an indication of energy consumption for the material used during grinding. The cement strength properties, the hardness and elastic modulus of the clinker depend on the raw materials, the kiln operating conditions and the type of fuels used.

The aim of this study is to evaluate the hardness and elastic modulus of the clinker mineral phases and their fracture strength during the comminution processes by instruments indentation. The influence of mineralogical, chemical and physical properties was carried out using several analytical techniques, such as: optical microscopy, X-ray diffraction with Rietveld refinement (XRD) and X-ray fluorescence (XRF). The drop weight test (DWT), commonly used for assessing the breakage characteristics of rocks, and the Bond ball mill grindability test were performed to characterize the mechanical properties of clinkers. The first test supplies the impact parameter "A.b", meaning the higher the impact parameter the lower the breakage strength. The Bond ball mill test provides the so-called standard work index (WI), defined as the specific power required (kWh/t) to reduce a material from a nominal infinite size to a P80 (80% of the material passing through a sieve aperture) size of 100 μm [2,3].

Instrumented indentation, also known as depth-sensing indentation or nanoindentation, is increasingly being used to probe the mechanical response of materials including metals and ceramics as well as polymeric and biological materials. The additional levels of control, sensitivity, and data acquisition offered by instrumented indentation systems have resulted in numerous advances in materials science, particularly regarding fundamental mechanisms of mechanical behavior at micrometer and even sub-micrometer length scales [4].

In this case study, the elastic modulus and the Vickers hardness of the major four mineral phases contained in commercial clinkers were measured by nanoindentation as well as the matrix inclusions

* Corresponding author.
E-mail address: vladiasouza@gmail.com (V.C.G. de Souza).

0008-8846/$ – see front matter © 2008 Elsevier Ltd. All rights reserved.
doi:10.1016/j.cemconres.2008.02.011

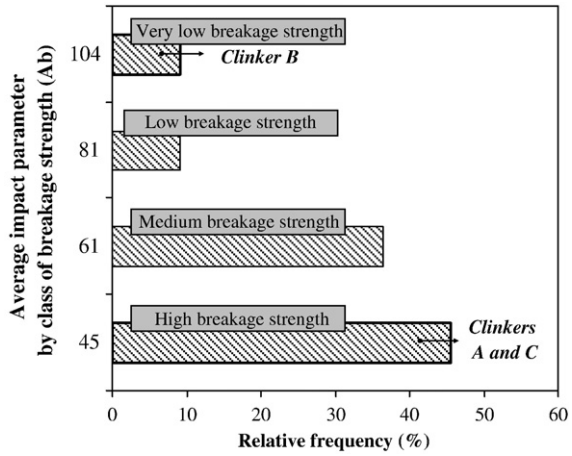

Fig. 1. Strength ranking of clinkers according to impact parameter by DWT tests.

(aluminates and ferrites) in the silicates. The influence of these parameters and the crystal's mineralogical properties on clinker grindability was investigated.

2. Sample selection and rock breakage tests

Clinker samples coming from different cement plants from Brazil (involving eleven kilns) were used in the comminution study. Five very narrow size fractions (−25.4+22.2 mm, −22.2+19.0 mm, −19.0+15.9 mm, −15.9+13.5 mm, −13.5+12.7 mm) and three inputs of specific energy levels (0.25; 0.5 and 1.0 kWh/ton) were selected to carry out the DWT tests.

The commercial clinkers showed a large range in impact parameter (42–106) according to the DWT results appearing in Fig. 1. Besides, Fig. 1, shows that the coarse nodules of commercial clinkers have generally medium (51<A.b<63) to very high (Ab<50) breakage strength. These intervals represent, in relative frequency, 36% and 45%, respectively, of the clinkers tested. Clinkers with low or very low breakage strength represent a minor group (relative frequency of 9%). From these results, three clinkers (A, B and C) were selected: (i) two high strength clinkers (A and C) and (ii) one very low strength clinker (B). After, clinkers A, B and C were submitted to the ball mill tests to determine the work index values.

Table 1 shows the WI results for clinkers A, B and C. Although clinker B has a high WI value (heavy grindability, classification according to Opoczky [5]) it showed very low breakage strength by DWT. On the other hand, clinkers A and C have high WI but they have also high breakage strength by DWT.

3. Sample preparation and experimental procedures

A mass of approximately 100 kg of clinker was homogenized and quartered to 5 kg aliquot used to determine nodule size distribution by screening. Three size fractions of nodules were selected and prepared (Table 2) following procedures suggested by Campbell and Centurione [7,8]. The size fractions chosen were then: 19.05×9.52 mm, 9.52×4.75 mm and 4.75×2.38 mm. Ten (10) nodules from the fraction 19.05–9.52 mm and ten (10) nodules from the fraction 9.52–4.75 mm

Table 1
Bond ball mill grindability test results

Clinker symbol	WI (kWh/t)	Classification
Clinker A	22.0	Hard grindability
Clinker B	19.8	Hard grindability
Clinker C	18.5	Hard grindability

Table 2
Clinker nodules size distribution

Fraction	Interval size (mm)	Weight %		
		A	B	C
1	>19.05	17.82	16.87	21.17
2	19.05–9.52	22.53	23.49	22.55
3	9.52–4.75	27.05	17.58	21.31
4	4.75–2.38	28.36	22.9	25.65
5	<2.38	4.24	12.77	9.32
	Total	100.00	100.00	100.00

were randomly chosen and mounted in twenty (20) polishing sections with 30 mm diameter. Thirty (30) nodules from the 4.75–2.38 mm fraction were mounted in three (3) polishing sections with 30 mm diameter (ten nodules by polishing section).

The specimens were cut using a diamond saw, removing the top and the bottom of the nodules. After, the specimens ("coins" of clinker) were impregnated with an epoxi resin of low viscosity to permeate the material's pore system. To speed the infiltration, the specimens were completely immersed in epoxy, and a vacuum applied to remove remaining air. Upon release of the vacuum, the epoxy was forced into the pore system. The epoxy was cured at ambient temperature for 24 h, and then was ready for grinding and polishing. Following some procedures suggested by Campbell [7], abrasive papers of 100, 220, 320, 400 and 600 (silicon carbide paper) were used with propylene glycol as lubricant in the grinding stages. Subsequent polishing stages of 6 μm to 0.25 μm with diamond polishing pastes were performed. Approximately 6 to 10 min for grinding or polishing each paper was normally sufficient, after which the sample was thoroughly cleaned with isopropyl alcohol in a sonic cleaner. The polished surfaces were protected with an acrylic spray after the microscopic analyses, which could be removed by gentle rubbing with an acetone- or xylene-soaked rag to be re-analyzed. The polished section surfaces were etched by Nital (1.5 mL of nitric acid, HNO_3 in 100 mL of isopropyl) superimposed on a 20-second potassium hydroxide etch which turns C_3A light brown and colors the silicates. The reflected light optical microscopy was used to characterize the different clinker samples.

One hundred of belite and alite crystals were measured in each polishing section and the average value was adopted as the crystal size described in this work. Description of the porosity, crystals shape, inclusions and microcracks in crystals represents the statistical result of detailed analyses of hundred crystals contained in twenty three (23) polishing sections of each clinker, totaling 69 polishing sections in this study.

X-ray Diffraction (XRD) with Rietveld refinement was applied to accurately quantify the phases present in the samples by using the same procedures adopted by Gobbo [9].

For the nanoindentation essays at least three additional polished sections were prepared for each clinker A, B and C. An extra sample for each clinker was cut in a 10 mm edge cubical form. These samples were polished again and analyzed by optical microscope to check the quality of polishing. This procedure was adopted to avoid the influence of the preparation, the substrate and setting conditions of the samples on the measurements of hardness and elastic modulus. Twenty indentations in each mineral phase were carried out and the Vickers hardness and elastic modulus average value were determined.

The procedures for nanoindentation tests followed ISO 14577 [10], which has been prepared to enable the user to evaluate the indentation of materials by considering the force and displacement during plastic and elastic deformation. By monitoring the complete cycle of increasing and removal of the test force, hardness values equivalent to traditional hardness values can be determined. More significantly, additional properties of the material, such as its indentation modulus and elastoplastic hardness, can also be determined. All these values

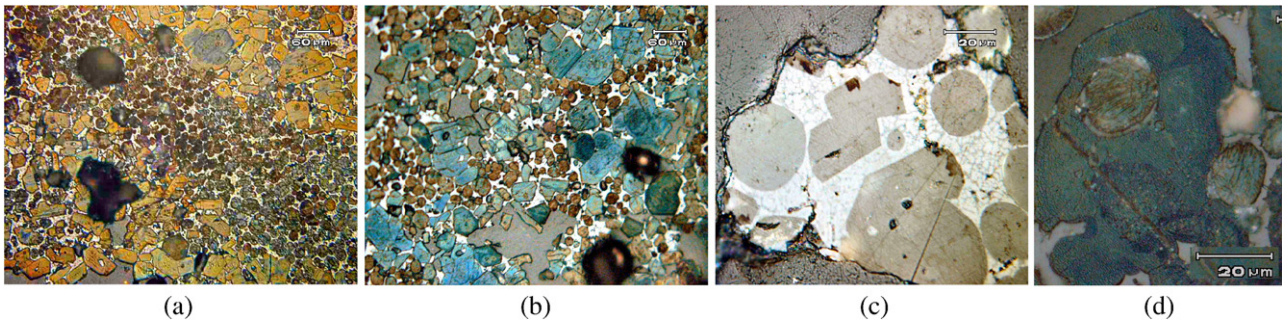

Fig. 2. Clinker A observed by optical microscope: (a) nodule of clinker and a large band of belites, type I belites (200×); (b) belites dispersed and subhedral alite crystals (200×); (c) round belites, type I belite (1000×) and (d) amoeboid or cannibalistic alite with inclusion of round belite (1000×).

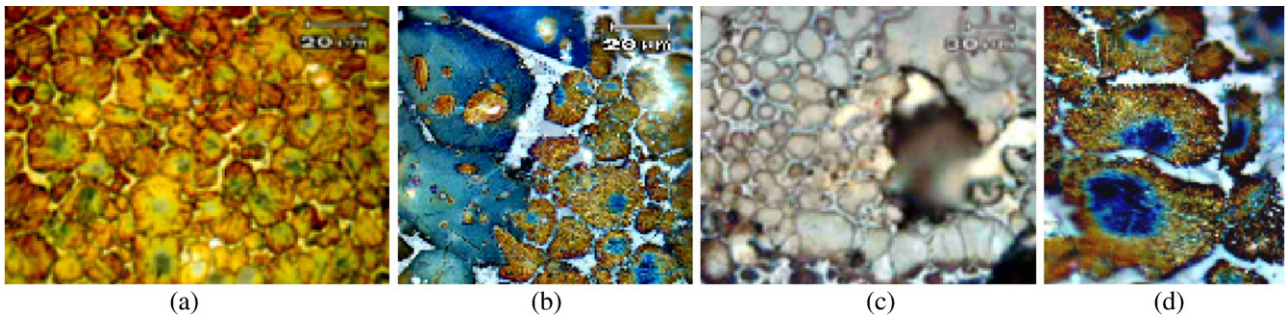

Fig. 3. The two types of belites in clinker B measured by HIT and observed by optical microscope: (a) ragged belites, type I belite (1000×); (b) ragged belites and belites inclusion in alites, type I belite (1000×); (c) coarser belites, type II belite (500×) and (d) zoom on belite, type I belite (1000×).

can be calculated without the need to measure the indentation optically. ISO 14577 specifies the method of instrumented indentation test for determination of hardness and other materials parameters.

The resolutions of load and displacement for the Fisherscope H100V equipment used were 0.02 mN and 2 nm, respectively. Hardness and elastic modulus were obtained using a Berkovich indenter, i.e., a three-sided pyramid diamond, with the same nominal area to depth relationships as the standard Vickers pyramid. The hardness instrument tests (HIT) were made with a maximum load of 45 mN and a total time load–unload cycle of 120 s. To prevent the load dependence on the hardness measurements, the indentation data was interpreted using the Doerner–Nix [11], Oliver–Pharr [12] and indentation size effect (ISE) theories [13]. The elastic modulus and hardness were measured at penetration depths of about 300 and 500 nm.

4. Experimental results

4.1. Optical microscopy

Clinker microscopy was used to distinguish between different types of belites (C_2S) and alites (C_3S), specifically to count the belite clusters and to estimate the average size of clusters and crystals. From the microscopy it was also possible to interpret the burning conditions [7].

Clinker A (Figs. 2 and 5a) depicts sub to anhedral (amoeboid) alite crystals of 60 μm (ranging from 15 to 120 μm), strongly zoned, twinned and cannibalistic alite crystals, without microcracks and with inclusions of belite. The belite crystals also show a large range in size distribution (8–63 μm), with an average of 22 μm. The majority of these crystals were rounded off without microcracking at the edges. The belites appear in clusters but also dispersed (Fig. 2a and b). The sample also shows a glass interstitial phase and porosity of around 23% (regular and isolated).

Clinker B (Figs. 3 and 5b) is constituted by subhedral alite crystals, with an average size of 29 μm (ranging from 11 to 77 μm), with abundant belite inclusions, and many alites are microcracked. There are several types of belites in this sample: ragged, some only with fingers and others with disorganized cores (denominated type I) and rounded off coarser belites (denominated type II). Both belite types have different nucleus coloration from the edges, but the type II belite is present in minor amount (minor than 2% by quantitative optical microscopy). The interstitial phase is comprised of semi-crystallized to

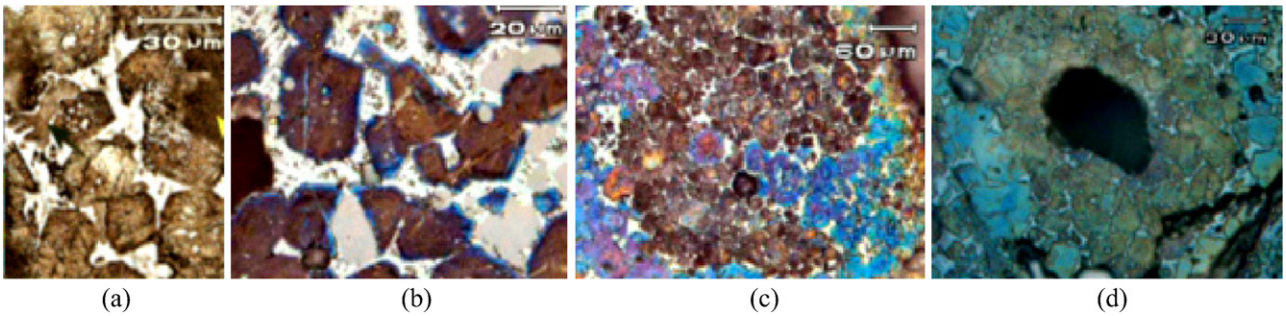

Fig. 4. Clinker C observed by optical microscope: (a) amoeboid belite (500×); (b) subhedral alite crystals with inclusions of matrix and MgO at the edges (1000×); (c) round type I belites in clusters (200×) and (d) round belites around pores (nests).

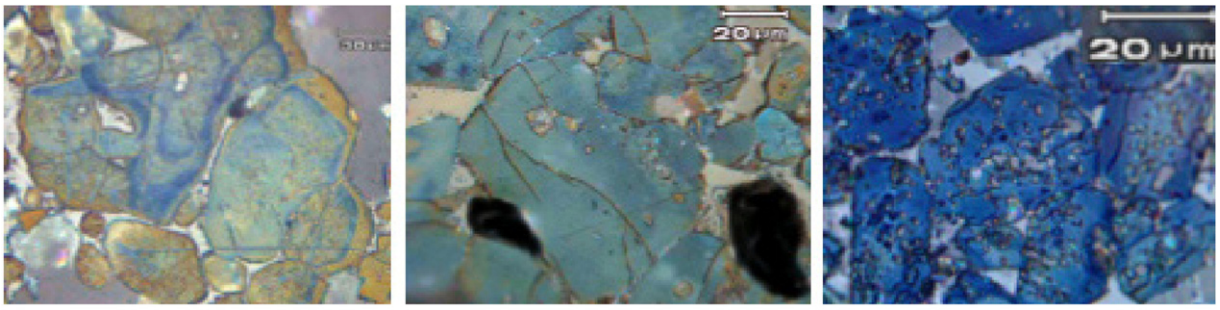

Fig. 5. Zoom on alites of the clinkers tested: (a) clinker A with cannibalistic, zoned and rounded (anhedral or amoeboid) alites (500×); (b) clinker B with microcracked alites (1000×) and (c) clinker C with abundant inclusions of matrix and MgO in alites (1000×).

crystallized minerals, as well as crystals of periclase developed in the matrix. Clinker B showed average porosity around 40%, as well as irregular and interconnected pores. Its characteristics were typical of clinkers showing a slow first cooling followed by a second cooling tending to slow.

Clinker C (Figs. 4 and 5c) shows subhedral alite crystals of 24 μm (ranging from 3 to 54 μm), cannibalistic, with matrix (abundant) and MgO inclusions. The belite crystals were almost rounded off (without fingers) in nests and clusters, and some were amoeboid and dispersed in the matrix. The interstitial phase of clinker C is semi-crystallized and the porosity is low (30%), with regular and interconnected pores.

The Fig. 5 shows the alites from clinkers A, B and C respectively. The shape of the alite crystals, the type and amount of inclusions in alites are very different in these three samples. Clinker A shows alite crystals with the largest size, rounded shape and zoning; clinker B shows alites microcracked with subrectilinear edges and a large size distribution; clinker C shows alites subhedral with abundant inclusions of matrix and MgO.

The description of belite clusters in clinkers A, B and C found in the coarse nodules tested by DWT (19.05×9.52 mm) is shown in Table 3.

Regarding Table 3, clinker C presents an average size of belite cluster larger than that found in clinkers B and A. Clinker B shows the highest maximum size of belite cluster (919 μm) and very high average counting of belite clusters by nodule (36 clusters by nodule). Clinker A shows the lowest average counting of belite clusters by nodule (13 clusters by nodule), but has a great number of dispersed and very rounded belites (60% from belites are dispersed).

Clinker A and, particularly, clinkers B and C, although featuring large (>150 μm) average size of belite cluster, produce blended cements according to the Brazilian mechanical and physical exigencies [6].

Table 3
Description of belite clusters in the clinkers analyzed by optical microscopy

Clinkers		A	B	C
Distribution (in percentage) and shape (between parenthesis) of the belite crystals	Regular clusters	15 (round)	55 (ragged) 15 (round)	80 (round)
	Irregular clusters	25 (round)	28 (ragged)	15 (round)
	Dispersed crystals	60 (round)	2 (ragged)	5 (round)
Average size of belite cluster (μm)		170	262	300
Minimum and maximum size of belite cluster (μm)		50–400	159–919	130–578
Average counting of belite clusters by nodule		13	36	20
Average size of belite crystals (μm)		25	20	22
Minimum and maximum size of belite crystals (μm)		3–53	8–72	8–63

4.2. X-ray Diffraction (XRD) and fluorescence (XRF)

The clinkers mineral composition determined by XRD is presented in Table 4. The alite content in clinker A is higher than in clinkers B and C. The belite content in clinker C is significantly lower than in clinkers A and B. Clinker A is the ferrite richest one. Clinker A presents only C_3A cubic and clinkers B and C present the two types of aluminates: C_3A orthorhombic and cubic. The largest differences are in the minor phases: periclase, free lime and arcanite. Clinker B has the lower content of arcanite, and two types of sulfates were detected in clinker A: arcanite and calcium langbeinite. Clinker A has the lowest free lime content, followed by clinkers C and B with 0.8 and 1.7% free lime content respectively.

The clinkers chemical ratios were estimated from oxides quantified by XRF (Table 5). The free lime was quantified by ethylene glycol method according to the NBRNM13 [14]. It was observed that clinker A presents a higher lime saturation factor (LSF) than B and C, but a lower silica ratio (SR). The alumina ratio (AR) can influence the grindability [6]; normally clinkers with a high AR have high grindability. AR values for the studied clinkers are 1.52 (clinker A), 1.57 (clinker B) and 1.46 (clinker C). TiO_2 and Mn_2O_3 contents were determined by XRF, and clinker A showed the highest values.

4.3. Nanoindentation

Small differences were observed in the hardness and elastic modulus values measured by the nanoindentation between the two types of samples tested: (i) round sections of 30 mm in diameter, and (ii) 10 mm edge cubical pieces. Vickers hardness and elastic modulus

Table 4
X-ray Diffraction results for studied clinkers (wt.%)

	A	B	C
Phase/sample			
C_3S	70.2	66.6	66.9
C_2S	13.3	12.3	7.9
C3A-cubic	2.6	3.0	1.3
C3A-orthorhombic	–	1.9	1.6
C_4AF	10.1	7.6	8.2
Periclase	0.6	6.4	11.2
Free lime	0.2	1.7	0.8
K_2SO_4[a]	1.7	0.5	2.1
$K_2Ca_2(SO_4)_3$[b]	1.3	–	–
Total	100.0	100.0	100.0
Relations			
C_3S+C_2S	83.5	78.9	74.8
C_3A+C_4AF	12.7	12.5	11.1
C_3S/C_2S	5.28	5.41	8.47

[a] Arcanite.
[b] Calcium langbeinite.

Table 5
X-ray fluorescence results for clinkers A, B and C (wt.%)

	A	B	C
SiO_2	21.50	20.87	19.85
Al_2O_3	4.70	4.05	3.75
Fe_2O_3	3.10	2.58	2.56
CaO	64.85	61.58	57.65
MgO	1.50	7.48	12.01
Na_2O	0.10	0.40	0.12
K_2O	1.10	1.10	1.36
TiO_2	0.25	0.12	0.12
SO_3	2.20	0.28	0.97
Mn_2O_3	0.10	0.05	–
LSF[a]	95.70	94.90	93.48
SR	2.76	3.15	3.15
AR	1.52	1.57	1.46
Free lime[b]	0.50	1.01	1.21
Alkalies equivalent	0.82	1.12	1.01

[a] Ignoring SO_3.
[b] Determined by ethylene glycol method.

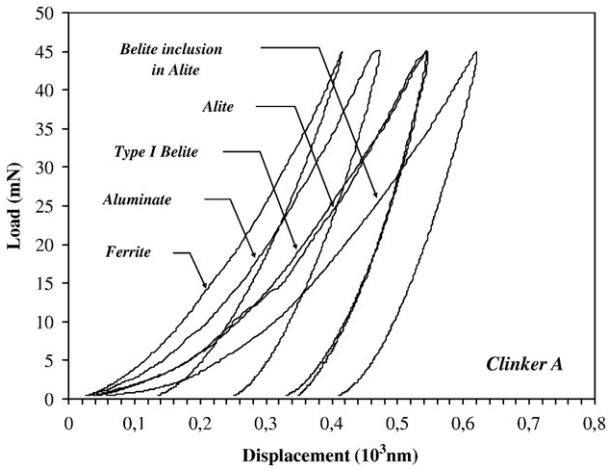

Fig. 6. Load–displacement curves of mineral phases of samples from clinker A.

average values for the mineral phases for clinkers A, B and C are shown respectively in Tables 6 and 7 (the round sections were identified as A, B and C and the cubical pieces were identified as A', B' and C').

The indentations number on inclusions of aluminate or ferrite inside alites from clinker A had to be reduced of twenty to five measures by polishing section, because the inclusions more common in this case were of type I belites.

The hardest phases were the ferrite (C_4AF) and the type II belite, followed by the aluminate (C_3A), alite (C_3S) and type I belite. Therefore, the type I belite shows the lowest plastic deformation strength (the lowest Vickers hardness).

Several factors influence the HIT measurements such as: distinctions between Vickers hardness measured from an indentation on a matrix inclusion (C_3A or C_4AF) inside silicate crystals and Vickers hardness measured from an indentation outside these inclusions. The mineral inclusions of aluminates or ferrites inside silicates showed an intermediate Vickers hardness value, which is between the value obtained for silicates and the value obtained for matrix phases.

Measurement deviations derive from several factors, such as crystal orientation, crystal chemical composition, substrate and parallelism problems in the polished section. Inclusions, pores, oxides, sulfates or free lime grains in the vicinity of the indentation performed on the crystal could also influence the measurements.

The standard deviation of the Vickers hardness values were high for the two types of belites found in the samples from clinker B (around 10.0% for type I belite and around 18.4% for type II belite).

The average values of elastic modulus for alites and type I belites ranged from 125 to 122 GPa, respectively (Table 7). These values are evidence of the larger plasticity of the silicates compared against the aluminate and ferrite phases. The last two phases show, respectively, an average elastic modulus of 139 and 142 GPa.

The elastic modulus of the alite in clinker A was smaller than the elastic modulus of the alite in clinkers C and B. This indicates that the alite in clinker A is more plastic than the alite in B and C. This is consistent with the Bond Index results.

The type II belite presents lower significantly fracture strength than the type I belite (Tables 6 and 7).

The aluminate of clinker A is more plastic than the aluminates of clinkers B and C (clinkers are based on their elastic modulus). The values of elastic modulus show, thus, a large difference in the mechanical behaviors of the matrix mineral phases (aluminates and ferrites) for all three tested clinkers.

Table 6
Average values Vickers hardness (GPa) and standard deviation, S.D. (%), of the minerals phases from clinkers A, B and C

Clinker	C_3S	S.D.	Type I C_2S	S.D.	Type II C_2S	S.D.	C_3A	S.D.	C_4AF	S.D.	Inc.*	S.D.
A	5.61	11.30	5.45	7.91	–	–	7.85	5.92	12.75	3.63	7.69	6.63
A'	5.59	11.11	5.53	6.72	–	–	8.76	6.04	12.86	3.11	7.49	3.37
B	5.86	5.56	5.85	10.38	12.56	19.58	8.10	5.00	10.04	5.00	6.51	5.72
B'	5.87	5.00	5.60	9.07	11.21	17.25	7.65	8.20	9.93	5.58	6.28	6.86
C	5.36	5.24	4.75	7.91	–	–	9.16	8.74	10.65	8.13	7.44	7.52
C'	5.83	6.56	4.77	7.18	–	–	9.02	6.35	10.46	8.67	6.57	7.76
Average global	5.69	7.46	5.33	8.20	11.89	18.42	8.42	6.71	11.12	5.69	7.00	6.31

Note: Inc.* C_3A or C_4AF inclusion in alites. S.D. (Standard Deviation).

Table 7
Average values of elastic modulus (GPa) of the minerals phases from clinkers A, B and C (GPa)

Clinker	C_3S	S.D.	Type I C_2S	S.D.	Type II C_2S	S.D.	C_3A	S.D.	C_4AF	S.D.	Inc.*	S.D.
A	112.79	10.06	117.48	11.33	–	–	124.39	2.47	135.92	2.41	124.19	2.80
A'	107.24	4.75	122.60	5.86	–	–	130.19	4.80	136.32	2.06	125.66	2.15
B	138.75	2.66	122.23	8.09	161.89	13.99	138.50	5.45	127.46	4.39	143.16	2.65
B'	130.81	6.28	124.52	9.92	162.60	9.09	144.48	6.35	128.24	4.17	140.90	4.48
C	129.32	4.86	117.27	9.02	–	–	149.11	4.31	165.13	7.73	130.56	4.55
C'	129.58	6.02	126.99	9.35	–	–	149.21	5.78	161.07	6.77	128.58	4.57
Average global	124.75	5.77	121.85	8.93	162.25	11.54	139.31	4.86	142.36	4.59	132.18	3.53

Note: Inc.* C_3A or C_4AF inclusion. S.D. (Standard Deviation).

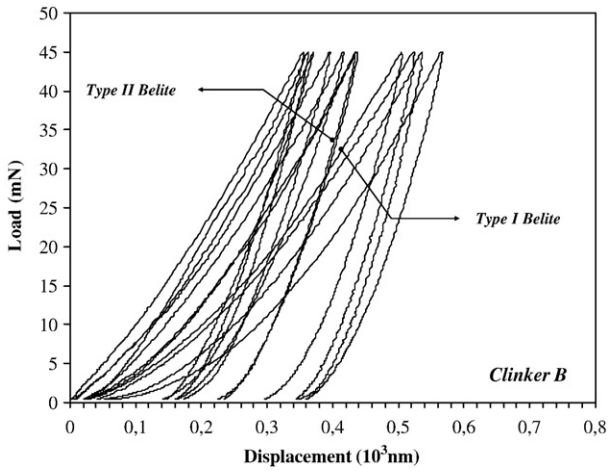

Fig. 7. Load–displacement curves of the belite phases of samples from clinker B.

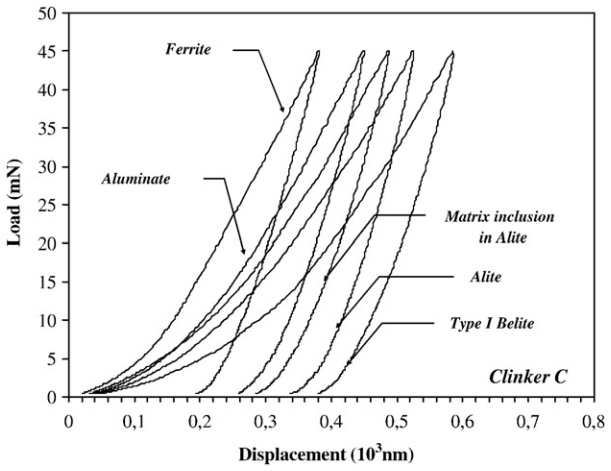

Fig. 9. Load–displacement curves of the mineral phases of samples from clinker C.

Figs. 6–9 show the mechanical behavior of the mineral phases in commercial clinkers through load–displacement curves. All of these anhydrous phases exhibit elastoplastic behavior. The matrix phase shows a non-pure elastic behavior while the silicates generally present a plastic behavior. These load–displacement curves shown in Figs. 6–9 represent the average curves by mineral phase and by clinker, calculated from all indentations made on polishing sections (round section or cubical piece).

Figs. 6 and 9 show that the load–displacement curves from one indentation made inside and outside one mineral inclusion (in alite crystals) are different. For example, when the indentation is made inside one inclusion with lower hardness, such as type I belite, the curve is displaced to the right of alite load–displacement curve made outside inclusion (Fig. 6). On the other hand, when the indentation is made inside one inclusion with higher hardness, such as one inclusion of C_3A or C_4AF, the curve is displaced to the left of alite load–displacement curve made outside inclusion (Fig. 9).

In Fig. 7, the differences in the mechanical behavior of the two types of belites (types I and II) in clinker B can be observed. The type I belite is more plastic than type II belite, the last with a higher Vickers hardness. Morphological differences between these two belite types were observed by optical microscopy (Fig. 3).

In Fig. 8, the ferrite of clinker B shows a sharp curve of unloading (near the pure elastic recovery) while the other phases present a behavior of plastic deformation.

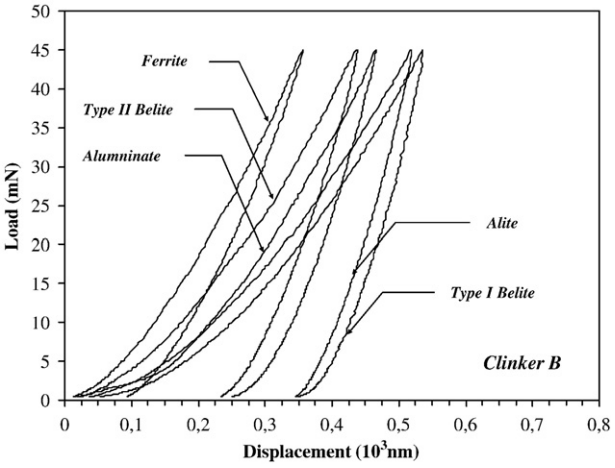

Fig. 8. Load–displacement curves of the mineral phases of samples from clinker B.

In Fig. 9, the belite crystals (type I) from clinker C shows a displacement curve to the right of the alite curve, evidencing a more plastic behavior.

The average Vickers hardness weighted, considering only the major four phases from XRD analysis (Table 4), produced results of approximately 6.2 GPa for clinker A, 6.0 GPa for clinker B (considering 10.5% of type I belite and 1.8% of type II belite) and 5.2 GPa for clinker C. The average elastic modulus was 110.2, 121.6 and 114.0 GPa for clinkers A, B and C, respectively.

5. Discussion

The crystals shape and size, as well as the “cannibalism” (crystals union), observed in alites or belites are one reflex of the clinker formation process and can be explained by Ostwald ripening [15]: mineral grain size and shapes spontaneously adjust toward a state of lower surface free energy. According to Best [15], large and small crystals of the same phase dispersed in a communicating fluid or melt at fixed pressure and temperature are relatively more and less stable, respectively, because of their differences in surface free energy per volume. Consequently, smaller crystals tend to be consumed at the expense of larger, more stable grains. The result of this equilibrating “ripening” is in an overall increase in average grain size of the system. Clinker A, with rounded shape and big size crystals, is a perfect example of this.

Clinker C shows some similarities with clinker A due the presence of some amoeboid belite crystals, cannibalistic alites and presence of belite clusters with size bigger than 150 μm. Both clinkers were thus probably submitted to high temperatures for long time. According to Hills [16], clinkers that show these characteristics present hard grindability. Observations on industrial practice also lead the authors to believe that clinkers submitted to a longer burning time are actually very hard to grind (high energy costs). On the other hand, this theory can very well explain why clinkers A and C show high WI and high fracture strength by DWT, but doesn't explain the behavior of clinker B.

It is necessary to remember that in the Bond tests the material must be previously crushed until it passes through a 3 mm sieve. The belite clusters with high hardness (as type II belites from clinker B) or made by ragged belites (as type I belites from clinker B) will have higher probability to be crushed prior to Bond ball mill test being conducted, due to the maximum grain size admitted for the WI experiment (3 mm), than rounded belites dispersed or in clusters. This explains better why clinker B features WI values higher or similar to those of clinkers A and C, but lower breakage strength by DWT (coarser nodules).

Besides, clinker A shows: (1) rounder and big belite and alite crystals and (2) highest C_3S and C_2S content. As the silicates present the lowest Vickers hardness values of the four major components of clinkers, clinker A showed the hardest grindability.

The Vickers hardness weighted values, considering only the major four phases from XRD analysis, indicate that clinker C should have the highest breakage strength, but in this calculation was not considered the Vickers hardness of the matrix inclusions in alites. If the inclusions of matrix in the silicates of clinker C, which are abundant, would be considered, the actual Vickers hardness of this clinker would be slightly higher. Thus, the three clinkers, A, B and C, in fact, contain crystals with high and similar fracture strength. This explains why the three clinkers tested showed high and similar work index values.

To explain the fracture mechanics of the coarser nodules of clinkers, it is necessary to analyze the DWT tests. DWT test could be more representative than WI as it uses the very last five narrow size fractions and three inputs of specific energy levels (kWh/t). It is able to reflect basically the macro characteristics of the coarser nodules of clinkers, such as porosity. In contrast, other mineralogical properties of clinkers seem to affect the DWT results, such as, belite clusters and microcracks in alites.

The ragged belite clusters, many microcracked alites and a higher porosity (irregular and interconnected pores) were factors that definitively may have contributed together to decrease the breakage strength of the coarser nodules of clinker B (impact parameter very high). The coarser belites (type II) in clusters, from clinker B, that show very high Vickers hardness, also helped to decrease the breakage strength of these coarser nodules.

Therefore, counting belite cluster or nests is not sufficient to evaluate or explain the fracture mechanics of clinker coarser nodules. It must be considered also the type of belites, their shape (round, ragged or dismembered), the amount and distribution of belites, and specially Vickers hardness of the mineral phases.

Besides, the periclase and free CaO content (determined by ethylene glycol) had negligible effect on fracture strength of the coarse nodules of the tested clinkers. On the other hand, WI values of the clinkers can be correlated with these components: clinker with higher free CaO and periclase content showed lower WI.

Regarding the nanoindentation results, there is another interesting point: Vickers hardness and elastic modulus of pure mineral phases such as C_3S and C_2S were previously determined in the literature by Velez et al. [1]. They concluded that there was little influence of minor elements in the hardness and in the elastic modulus, although the load–displacement curves had shown a large difference between pure phases and impure phases. Tables 6 and 7 show the Vickers hardness and elastic modulus of mineral phases at commercial clinkers. These results are really different from those of the pure phases determined in prior literature [1], due to the presence probably of certain trace elements that will be object of further study. According to Opczky [5], the incorporation of the trace elements may affect: the micro symmetry and electrostatic relations of the structure of clinker minerals, the chemical bonds (covalent, ionic) between the ions, the coordination of ions and certain physical–mechanical properties (hardness, rigidity) of the clinker minerals. The change in the grindability of clinkers is the macroscopic manifestation of these effects. This could even explain differences in Vickers hardness and elastic modulus values for the same mineral phase among several commercial clinkers.

The shape of the unloading curve showed that the ferrite presents more elastic recovery behavior than the aluminates, while the silicate phases present a behavior next to plastic deformation. The main differences of Vickers hardness and elastic modulus are in the matrix and belite phases. The load–displacement curves from indentation on samples of clinker B show the possibility of the coexistence of belites with distinct mechanical behaviors in the same clinker. These belites will be object of further studies.

6. Conclusions

The most important evidence obtained from HIT results is that silicates (especially belites) are more susceptible to plastic deformation and, for this reason, can produce crack deviation that would propagate in the clinkers nodules. Coarse nodules of clinker with high porosity, if they contain these ragged belite clusters or microcracked alites, will present very low breakage strength in the first chamber of cement mills.

On the other hand, the same clinker, in the second chamber cement mill (fine grinding), not necessarily will show easy grindability. This happens with samples from clinker B, in fact, which showed the lowest fracture strength under impact by DWT, but also very high WI value.

The small differences in WI are related to mineralogical and mechanical properties of the mineral phases of commercial clinkers. The largest differences among the samples tested in DWT (clinkers A, B and C) are associated with macro characteristics of clinkers, such as porosity and belite clusters.

The Bond and DWT tests together may be used for explaining the resistance to breakage of clinkers and the influence of their chemical, physical and mineralogical characteristics on grinding, especially in multi chamber cement mills. HIT can supply additional information on the breakage mechanisms of the industrial clinkers, and was used in the present work specially to show that silicates really have more easy plastic deformation than aluminates or ferrites.

Acknowledgements

The authors thank the financial support from CNPq — Conselho Nacional de Desenvolvimento Científico e Tecnológico, Brazil and Cimbagé (CIMPOR — Cimentos de Portugal).

References

[1] K. Velez, S. Maximilien, D. Damidot, G. Fantozzi, F. Sorrentino, Determination by nanoindentation of elastic modulus and hardness of pure constituents of Portland cement clinker, Cem. Concr. Res. 31 (2001) 555–561.
[2] F.C. Bond, The third theory of comminution, Trans. Soc. Min. Eng. AIME 193 (1952) 484–494.
[3] T.J. Napier-Munn, S. Morrell, R.D. Morrison, T. Kojovic, Mineral Comminution Circuits — Their Operation and Optimisation, JKMRC, Austrália, 1996.
[4] M.R. VanLandingham, Review of instrumented indentation, J. Res. Natl. Inst. Stand. Technol. 108 (2003) 249–265.
[5] L. Opoczky, V. Gável, Effect off certain trace elements on the grindability of cement clinkers in the connection with the use of wastes, Int. J. Miner. Process. 74S (2004) S129–S136.
[6] NBR5736, Pozzolanic Portland Cement — Technical Standards Brazilian Association (ABNT), 1991.
[7] D.H. Campbell, Microscopical Examination and Interpretation of Portland Cement and Clinker, 2nd ed.Portland Cement Association, Skokie, I.L., USA, 1999.
[8] S.L. Centurione, Influência das características das matérias-primas no processo de sinterização do clínquer Portland, Master dissertation, Universidade de São Paulo, Brazil, 1993.
[9] L.A. Gobbo, L. Sant', L. Garcez, C_3A polymorphs related to industrial clinker alkalies content, Cem. Concr. Res. 34 (2004) 657–664.
[10] ISO 14577-1, Metallic materials — Instrumented indentation test for hardness and materials parameters — Part 1: test method, Int. Org. for Stand., 2002.
[11] M.F. Doerner, W.D. Nix, A method for interpreting the data from depth-sensing indentation instruments, J. Mater. Res. 1 (1986) 601–609.
[12] W.C. Olivier, G.M. Pharr, An improved technique for determining hardness and elastic modulus using load and displacement sensing indentation experiments, J. Mater. Res. 7 (1992) 1564–1583.
[13] P.C. Jindal, D.T. Quinto, Load dependence of microhardness of hard coatings, Surf. Coat.Technol. 36 (1988) 683–694.
[14] NBRNM13, Portland Cement, Chemical Analyses, Determination of Free Lime by Ethileno Glycol Method, Technical Standards Brazilian Association (ABNT), 2004.
[15] M.G. Best, Igneous and Metamorphic Petrology, 2nd ed.Blackwell Science Ltd, UK, 2003.
[16] L.M. Hills, Under the microscope — an introduction to clinker microscopy, Cem. Am. (1999) 39–43.